Electrical Conduction in Canine Pulmonary Veins
Electrophysiological and Anatomic Correlation

Mélèze Hocini, MD; Siew Y. Ho, PhD; Tokuhiro Kawara, MD; André C. Linnenbank, PhD; Mark Potse, MS; Dipen Shah, MD; Pierre Jaïs, MD; Michiel J. Janse, MD; Michel Haïssaguerre, MD; Jacques M.T. de Bakker, PhD

Background—Paroxysmal atrial fibrillation in patients is often initiated by foci in the pulmonary veins. The mechanism of these initiating arrhythmias is unknown. The aim of this study was to determine electrophysiological characteristics of canine pulmonary veins that may predispose to initiating arrhythmias.

Methods and Results—Extracellular recordings were obtained from the luminal side of 9 pulmonary veins in 6 Langendorff-perfused dog hearts after the veins were incised from the severed end to the ostium. Pulmonary veins were paced at the distal end, the ostium, and an intermediate site. During basic and premature stimulation, extracellular electrical activity was recorded with a grid electrode that harbored 247 electrode terminals. In 4 hearts, intracellular electrograms were recorded with microelectrodes. Myocyte arrangement immediately beneath the venous walls was determined by histological analysis in 3 hearts. Extracellular mapping revealed slow and complex conduction in all pulmonary veins. Activation delay after premature stimulation could be as long as 96 ms over a distance of 3 mm. Action potential duration was shorter at the distal end of the veins than at the orifice. No evidence for automaticity or triggered activity was found. Histological investigation revealed complex arrangements of myocardial fibers that often showed abrupt changes in fiber direction and short fibers arranged in mixed direction.

Conclusions—Zones of activation delay were observed in canine pulmonary veins and correlated with abrupt changes in fascicle orientation. This architecture of muscular sleeves in the pulmonary veins may facilitate reentry and arrhythmias associated with ectopic activity. **(*Circulation*. 2002;105:2442-2448.)**

Key Words: fibrillation ■ veins ■ mapping ■ electrophysiology ■ action potentials

The concept of multiple wavelet reentry as a mechanism for atrial fibrillation was proposed by Moe and Abildskov[1] in 1959 and experimentally confirmed by Allessie and coworkers[2] in 1985. Multiple wave fronts throughout the atrium maintain themselves by reentry around continuously shifting areas of functional conduction block. Although multichannel mapping of atrial fibrillation in humans suggests the same mechanism in human hearts, evidence is increasing that in most patients, paroxysmal atrial fibrillation is initiated by focal sources. These usually are located in the pulmonary veins and can be treated successfully by discrete radiofrequency energy applications.[3] The mechanism of arrhythmogenicity in the pulmonary veins is unknown. The purpose of the present study was to determine those electrophysiological and histological characteristics of the canine pulmonary veins that may facilitate the occurrence of local arrhythmias.

Methods

Measurements were made on isolated, blood-perfused hearts obtained from 6 mature mongrel dogs (2 to 4 years old of either sex and weighing 20 to 30 kg). Procedures conformed to institutional guidelines.

Preparation of Hearts

The methods of preparation and perfusion of isolated hearts have been described elsewhere.[4] Briefly, after deep anesthesia, the heart was excised and the aortic root cannulated to permit Langendorff perfusion. Hearts were perfused (flow 200 to 300 mL/min) with a mixture of blood (50%) and Tyrode's solution.

Extracellular Recordings

Mapping of the extracellular electrical activity of the pulmonary veins was performed in 6 canine hearts. Pulmonary veins were incised from the distal end to the ostium, spread open with the inner surface facing upward, and pinned to a silicon rubber support. Then, electrical stimulation was performed, and unipolar recordings were made from the luminal side of the pulmonary veins with a multiter-

Received December 4, 2001; revision received February 27, 2002; accepted February 28, 2002.

From Hôpital Cardiologique du Haut-Lévèque (M. Hocini, D.S., P.J., M. Haïssaguerre), Pessac, France; Paediatrics, National Heart & Lung Institute, Imperial College School of Medicine (S.Y.H.), London, UK; the Experimental and Molecular Cardiology Group, Cardiovascular Research Institute Amsterdam (T.K., M.J.J.) and the Department of Medical Physics (A.C.L., M.P.), Academic Medical Center, Amsterdam, the Netherlands; and the Interuniversity Cardiology Institute of the Netherlands (J.M.T.d.B.), Utrecht, the Netherlands.

Correspondence to Jacques M.T. de Bakker, PhD, Department of Experimental Cardiology, Academic Medical Center, Meibergdreef 9, 1105 AZ Amsterdam, The Netherlands. E-mail j.m.debakker@amc.uva.nl

Circulation **is available at http://www.circulationaha.org** **DOI: 10.1161/01.CIR.0000016062.80020.11**

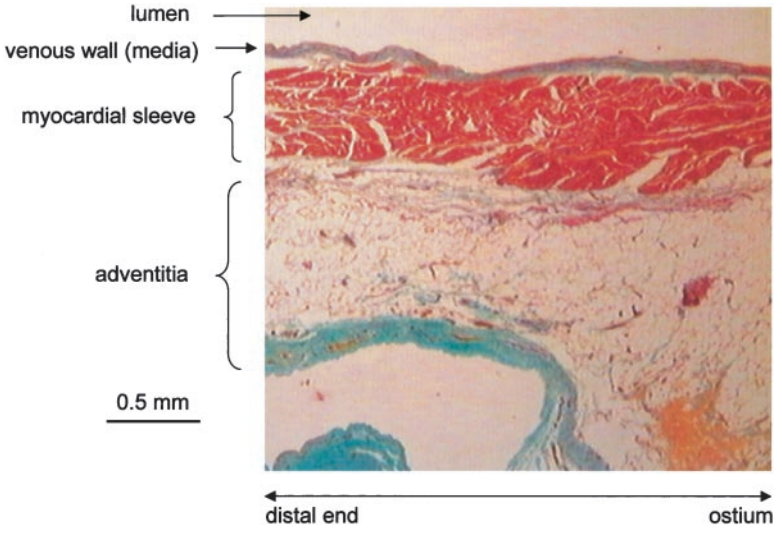

Figure 1. Section from left inferior pulmonary vein. Trichrome staining.

minal grid electrode that harbored 247 terminals (silver wires, diameter 100 μm, arranged in a 19×13 matrix at interelectrode distances of 300 μm). The multielectrode was mounted in a micromanipulator. Corners of the electrode were marked with fine pins in the tissue.

Recordings were obtained during sinus rhythm, during stimulation at a basic cycle length (BCL) of 500 ms, and after premature stimuli. The latter were delivered every eighth beat at coupling intervals ranging from 400 ms down to the refractory period in steps of 10 ms. Electrograms were amplified 40 times (noise level 3 μV, peak to peak), band-pass filtered (0.1 to 500 Hz), and digitized at 16 bits.

Analysis was performed with MatLab software (The MathWorks Inc). The point of maximal negative dV/dt for each electrogram was selected as the time of local activation. To check for local deflections, we determined the Laplacian by subtracting the electrogram recorded at an electrode and the weighted sum of signals recorded at adjacent electrodes. The Laplacian suppresses remote activity but resembles a unipolar recording. Isochronal lines were drawn every 2 ms. Isochronal crowding and complex, fragmented electrograms were considered to indicate zones of slow conduction, whereas double potentials widely separated (>30 ms) by an isoelectrical line were assumed to be generated by areas of conduction block. Activation delay was defined as the difference between earliest and latest activation within the recording area.

Stimulation Protocol

Recordings with the 247-point multielectrode were made during pacing from the right atrium and 3 sites in the pulmonary veins: the ostium, the distal end, and an intermediate site. The multielectrode was placed at 2 positions: one ostial and the other at the distal end of the pulmonary veins.

Bipolar pacing electrodes consisted of 2 silver wires (diameter 0.1 mm, interelectrode distance 0.2 mm) isolated except at the tips. Stimulus strength was 2 times current threshold, and pulse width was 1 ms.

Intracellular Recordings

In 4 hearts, microelectrodes were impaled at 3 different levels of the pulmonary veins at sites on a line along the veins: the ostium, the distal end, and an intermediate site. Characteristics of the action potentials were determined during stimulation at a BCL of 500 ms. To study the vulnerability to delayed afterdepolarizations, burst pacing was applied for 10 seconds at a cycle length of 250 ms after 50 μg of norepinephrine and 50 μg of ouabain were added sequentially to the perfusate. Action potential duration was calculated at 50% of the maximal amplitude.

Because it is not possible to achieve stable microelectrode impalements in blood-perfused mammalian hearts owing to vigorous cardiac contractions, 1 to 2 g of diacetyl monoxime was added to the perfusate to dampen cardiac contractions. Diacetyl monoxime in the concentration of 10 to 20 mmol/L has a markedly negative inotropic effect but has little effect on the action potential.[5]

Histological Investigation

Histology was performed on 3 canine hearts randomly selected from those in which extracellular pulmonary vein mapping was performed. Pins were replaced by India ink markers, and veins were processed for routine histology. Serial sections (10 μm thick) were cut parallel to the long axis of the veins and perpendicular to the vessel wall. Every tenth section was mounted on glass slides and stained with a modified Masson's trichrome technique. India ink markers facilitated identification of the mapped area. The main orientation of myocyte bundles on the luminal aspect of the veins was reconstructed manually on scaled diagrams with the ink markers as reference points. Areas devoid of myocytes were noted.

Statistical Analysis

Results are expressed as mean±SD. Mean values were compared by χ^2 test. Results were considered significant at $P<0.05$.

Results

Histology

All veins showed comparable arrangement of the components of the vessel wall, ie, endothelium, media, muscular sleeve, and adventitia. Sleeves of myocardial cells similar to striated atrial myocytes were located between the media and adventitial layers of the vessel wall (Figure 1). The media was thin, ranging from 0.1 to 0.3 mm thick, and consisted of fibrous and elastic tissue and smooth muscle cells. The myocardial sleeves were thickest close to the ostia, measuring 0.5 to 0.8 mm in thickness, but they tapered and disappeared toward the lung hila. The outermost layer, the adventitia, mainly comprised fibrous, elastic, and fatty tissues. Its thickness varied considerably, but it was generally greater than that of the media and the myocardial sleeve together.

The myocytes closest to the luminal aspect of the vein were often haphazard in arrangement, with fibers arranged in multiple directions and abrupt changes in the arrangement, as shown at the ostial positions of the recording electrode in Figure 2. This figure is a schematic of the fiber arrangement in a left superior (A) and left inferior (B) pulmonary vein. The pattern of longer, aligned fibers was often interrupted by

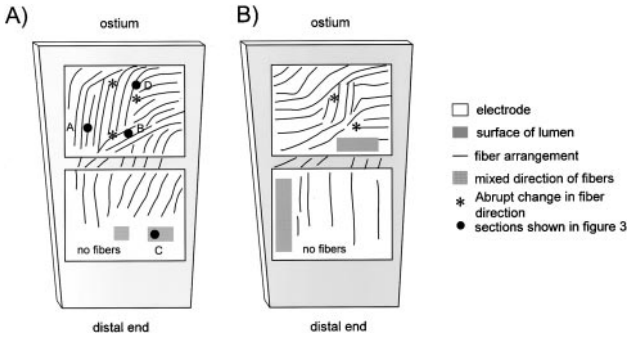

Figure 2. Reconstruction of fiber orientation at recording sites in left superior (A) and left inferior (B) pulmonary vein. Fiber orientation at ostial recording site is complex, showing areas with sudden change in fiber orientation and areas with mixed fiber orientation. At distal end, myocardial fibers run more or less parallel to long axis of vein and are often sparse. A through D in panel A indicate sites from which sections in Figure 3 were taken.

areas with short fibers oriented in mixed directions (hatched area in upper recording area of Figure 2B).

At the distal end of the veins, myocardial fibers generally ran in the longitudinal direction, but areas with mixed fiber direction were present as well. In this part of the veins, fibers were often sparse or even absent.

Sections from 4 sites (A through D) in the pulmonary vein shown in Figure 2A that revealed different arrangements of myocardial fibers are shown in Figure 3. Sections were parallel to the long axis of the veins and perpendicular to the vessel wall. Myocytes stained reddish; areas at the right of the sections that stained gray/purple marked the venous wall closest to the lumen (E). Interstitial fibrosis was present in a number of sections (gray zones between myocytes). The longitudinal appearance of the myocardial cells in Figure 3A (open arrow) points to an orientation parallel to the long axis of the pulmonary vein. The same orientation of myocardial fibers is shown schematically in Figure 2A (site A). The round forms in the upper part of Figure 3B are cross sections of myocyte bundles (arrow), where fibers ran perpendicular to the long axis of the veins. The lower left part of this section shows elongated myocardial cells (double arrow), which indicates a profound change in fiber direction. In Figure 3C, myocardial fiber orientation in deep layers was parallel to the long axis of the vein (open arrow at left). However, orientation of myocardial cells directly underneath the media was mixed; cells oriented nearly parallel to the vein axis (open arrow at right) alternated with myocytes that lay perpendicular to the long axis (solid arrow). Figure 3D illustrates a sudden change in fiber orientation. Myocardial cells in the upper part of the section were oriented along the long axis of the vein (open arrow), whereas in the lower part, cells were nearly perpendicular to it (solid arrow).

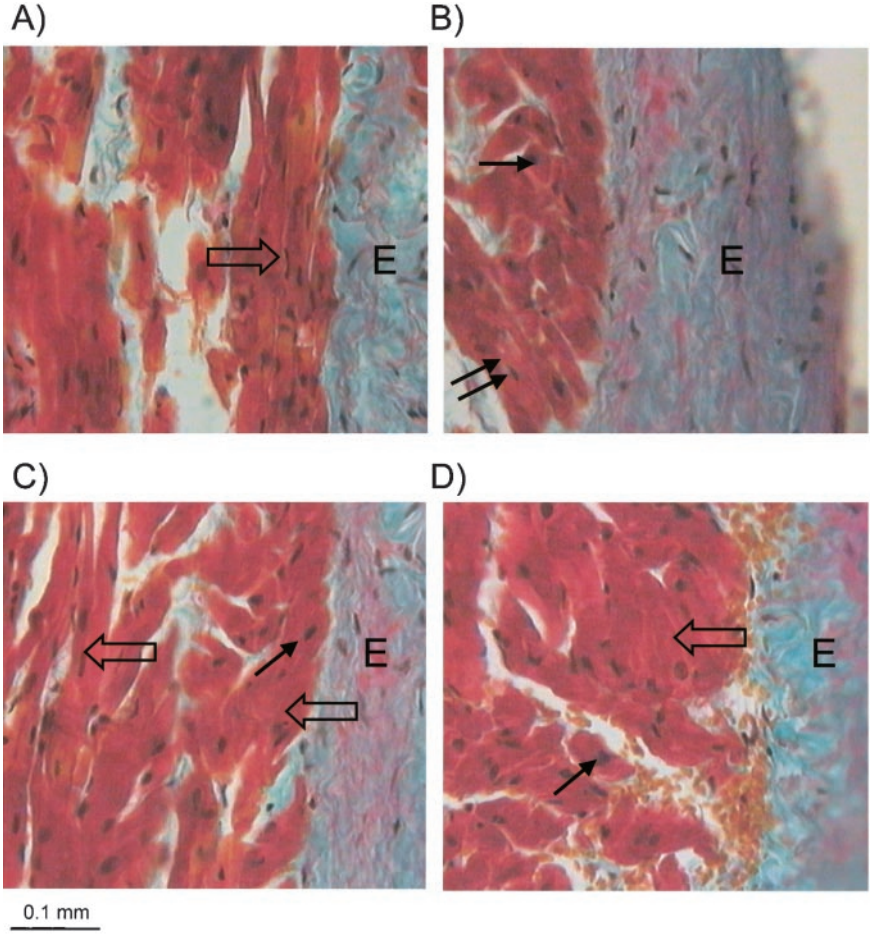

Figure 3. Sections from 4 sites of left pulmonary vein in Figure 2. Venous wall stains gray/purple, whereas myocytes stain reddish. Sections are parallel to vein axis and perpendicular to vessel wall. Sections were taken from locations shown as dots (A, B, C, and D) in Figure 2A. Open arrows point to myocyte orientation parallel to vein axis, solid arrows to orientation perpendicular to this axis. Double arrow in panel B shows myocyte orientation that deviates 45° from longitudinal direction.

Activation Delay Between Earliest and Latest Activated Site Within Recording Area During BCL of 500 ms (Delay at BCL) and After Premature Stimulus That Exceeded the Refractory Period (Delay at RP) by 2 ms

	RA Stimulation (n=5)	PV Ostium Stimulation (n=7)	Distal PV Stimulation (n=5)	Mid PV Stimulation (n=4)
Delay at BCL, ms	14±6.8	19.1±10.6	18.2±10.4	36.8±2.1
Delay at RP, ms	17.6±7.3	35.9±28.2	37.0±7.3	78.7±14.1
Increase in delay, ms	3.6±3.9	16.7±23.3	18.8±10.9	42.0±16.1

RP indicates refractory period; RA, right atrium; PV, pulmonary vein; and n, number of pulmonary veins investigated.

Electrophysiological Characteristics

Mapping of endocardial electrical activity in the pulmonary veins was performed in 6 hearts. Nine pulmonary veins (4 right superior veins, 3 left superior veins, and 2 left inferior veins) were studied. Areas revealing myocardial sleeves showed multiple deflections generated by local activation of the sleeves and remote atrial activation. The Table shows mean activation delay in the recording area (4×6 mm) at baseline and during premature stimulation from 4 different sites. The shortest activation delay was observed during basic and premature stimulation from the right atrium. The longest activation delay was obtained during pacing from the middle of the pulmonary veins (up to 120 ms after premature stimulation). Activation delay was similar during stimulation from the ostial and distal ends of the pulmonary vein.

Zones of conduction delay (delay between adjacent sites, 0.3 mm apart, >3 ms) were found in all pulmonary veins. Figure 4A shows different characteristics of the zones of activation delay. Lengths of these zones and the amount of delay were greater in the left inferior and right superior pulmonary veins than in the left superior pulmonary vein.

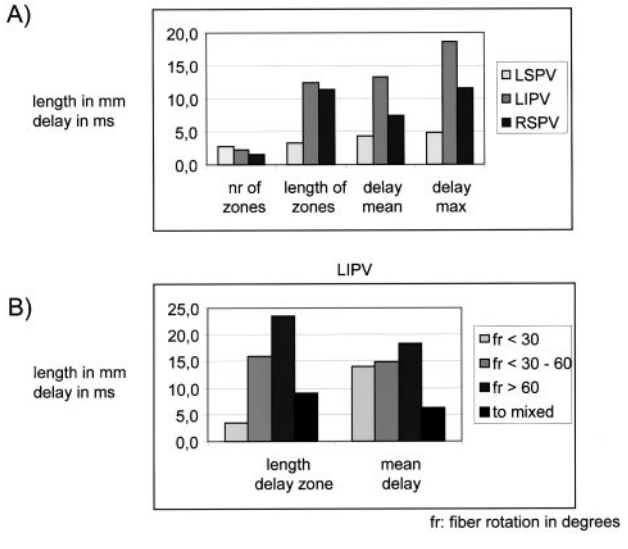

Figure 4. A, Characteristics of zones of activation delay for different pulmonary veins. B, Length of zone and mean delay along zones of conduction delay in left inferior pulmonary veins, depending on fiber rotation at site of delay. LSPV indicates left superior pulmonary vein; LIPV, left inferior pulmonary vein; RSPV, right superior pulmonary vein; and nr, number.

"Local" fractionation was found along the zones of conduction delay. On average, 2.2 zones of fractionated electrograms (length of zones ≥0.6 mm) were found in the pulmonary veins during basic stimulation.

Electrophysiological and Histological Correlation

Zones of activation delay and conduction block in the activation maps were generally related to sudden changes in fiber direction. To quantify the correlation between electrophysiological and histological data, we determined the change in fiber direction or texture at the zones of conduction delay in the direction of wave-front propagation. Four classes were distinguished: (1) fiber rotation <30°, (2) fiber rotation between 30° and 60°, (3) fiber rotation >60°, and (4) change to mixed fiber direction. The length of the zones of delay and the mean delay along the zones increased with the amount of fiber rotation in all pulmonary veins (Figure 4B). Zones of delay where fibers changed to a mixed texture revealed lower values for both the length of the zone and the mean value of delay.

An example of the relation between electrophysiological and histological characteristics is given in Figure 5. This figure shows activation patterns recorded near the ostium of a right superior pulmonary vein during stimulation at a BCL of 500 ms (A) and after premature stimulation with a coupling interval of 135 ms (B). The pacing electrode was located at the ostium of the pulmonary vein. During basic stimulation, the recording area was activated within 26 ms. Isochronal lines between 4 and 10 ms were widely separated, which suggests normal conduction during this interval. Subsequently, isochronal lines became more crowded, particularly as they approached recording site c (18-ms isochrone), which revealed a zone of slow conduction in this area. Activation delay was reflected by a closely coupled double deflection in electrogram c; the first deflection, marked ①, was caused by the wave front approaching the recording site, whereas the second deflection, ②, was the local deflection of the wave front distal from the zone of delay. The third complex, ③, was remote and caused by receding activation in the atrium. Local fractionation at site c, which reflected the zone of conduction delay, is better seen in the Laplacian signals in Figure 5D. The Laplacian signals in a and b show 1 local deflection. In contrast, the Laplacian signal in c reveals the local deflections at both sides of the line of delay. This zone of conduction delay corresponds to an abrupt

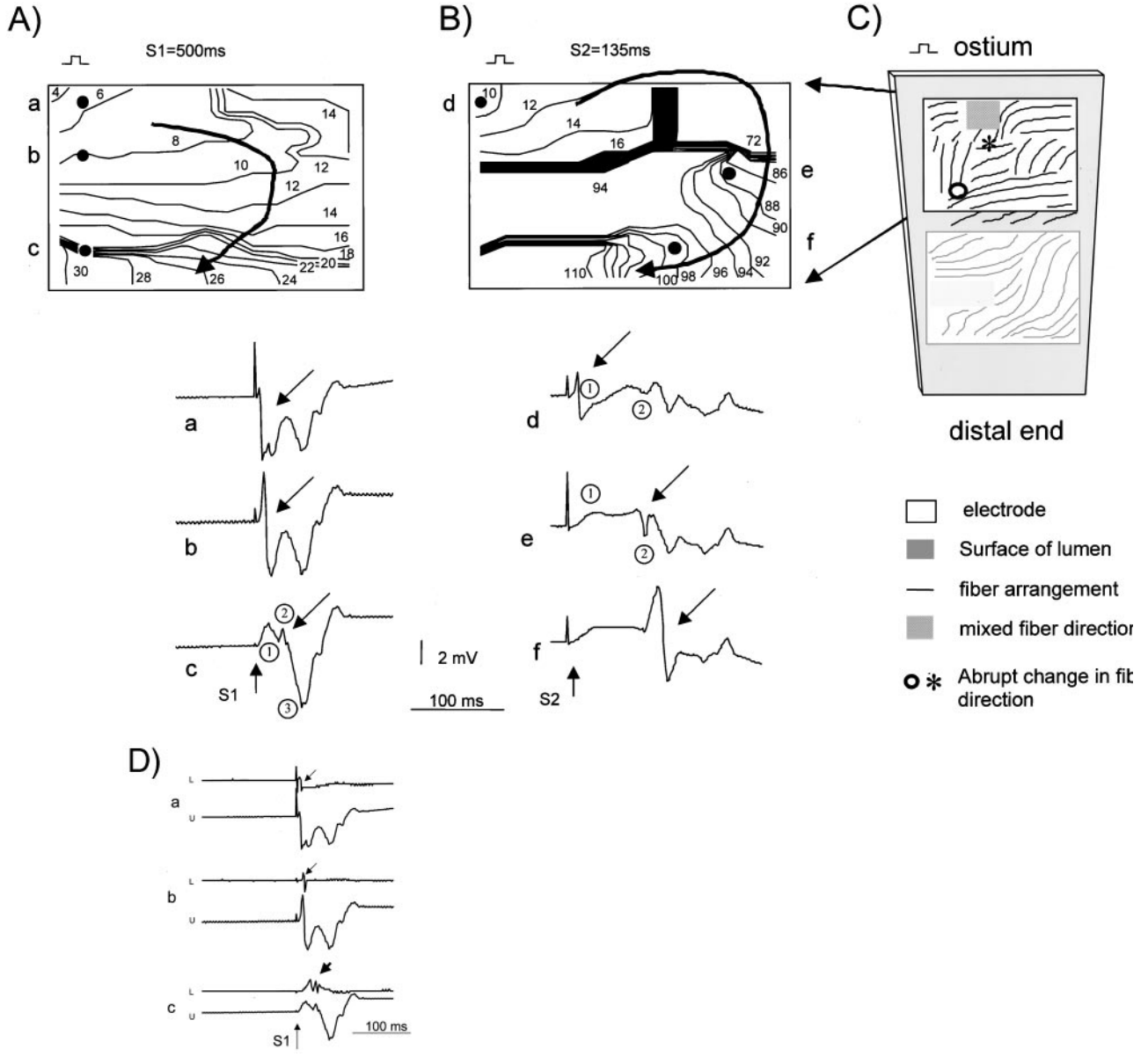

Figure 5. Activation maps of right superior pulmonary vein of canine heart during basic (A) and premature (B) stimulation at pulmonary vein ostium. Numbers are activation times determined relative to stimulus. Lines are isochrones, drawn every 2 ms. Arrows indicate dominant direction of activation. Unipolar electrograms a to f were recorded at sites indicated by black dots in maps. Arrows in tracings point to deflections that were generated by local activation. C, Fiber orientation in pulmonary vein at ostial position of multielectrode. S1 indicates basic stimulus; S2, premature stimulus. D, Unipolar and Laplacian signals during baseline stimulation at sites a, b, and c. L indicates Laplacian signal; U, unipolar electrogram.

change in fiber direction from vertical to almost horizontal, as shown in Figure 5C (open circle).

After premature stimulation at a coupling interval of 135 ms, the recording area was activated in 101 ms (Figure 5B). Starting at the upper left corner, activation proceeded toward the center of the electrode but was arrested by a zone of conduction block after 16 ms. Conduction block was suggested by the compact isochronal lines in that zone. This is the same zone in which isochronal lines became more crowded during basic stimulation. The zone of block is reflected in electrograms d and e by double potentials marked ① and ②. Arrows in the tracings point to local deflections, which were separated from the remote components (② for tracing d, ① for tracing e) by ≈80 ms. Sudden changes in fiber arrangement and mixed direction of fibers at the asterisk in Figure 5C could well be responsible for this zone of conduction block.

Between 16 and 72 ms, the activation front proceeded outside the recording area. Activation entered the right border of the recording area again after 72 ms and propagated toward the lower left corner of the recording electrode. Electrograms recorded in the center of the recording electrode revealed identical activation times (94 ms), which suggests an electrotonic origin. Activation block into this area could be related to the change in fiber direction just to the left of site e.

	ostium	middle	distal end
number of cells	N=14	N=8	N=13
amplitude (mV)	97 ± 17	99 ± 17	91 ± 10
dV/dt (V/s)	122 ± 66	120 ± 154	99 ± 46
APD_{50} (ms)	62 ± 15	66 ± 21	46 ± 25

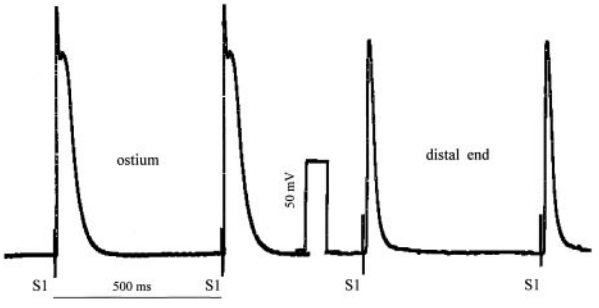

Figure 6. Upper panel, Characteristics of action potentials recorded at 3 levels (ostium, intermediate, and distal end) in 3 pulmonary veins during stimulation at ostium. Lower panel, Tracings are action potentials recorded at ostium and distal end of pulmonary vein. S1 indicates basic stimulus; APD_{50}, the action potential duration at 50% of the action potential amplitude.

Microelectrode Recordings

Figure 6 shows the characteristics of action potentials recorded in 35 cells in the pulmonary veins of 4 canine hearts (left inferior [7], right inferior [2], right superior [13], and left superior [13]). The action potential upstrokes were rapid (mean 114 V/s) and had large amplitudes (mean 96 mV). There was a tendency ($P=0.06$) for shorter action potential durations (62 versus 46 ms) and slower upstroke velocities (122 versus 99 V/s) at the distal end than at the ostium, although this difference failed to reach statistical significance. Two different types of action potentials were observed: action potentials with a distinct plateau (48%) and triangular action potentials without a plateau (52%). Statistically ($P=1.0$), there was no difference in action potential configuration between ostium and apex, although data suggested a tendency toward action potentials without a plateau at the apex. None of the cells impaled showed any diastolic depolarization. Burst pacing of the pulmonary veins and/or norepinephrine or ouabain did not produce afterdepolarizations.

Discussion

This study describes conduction properties in canine pulmonary veins and their correlation with myocardial arrangement.

Nonuniform Anisotropy

During premature stimulation, mean activation delay ranged from 17.6 to 78.7 ms, and activation frequently curved around zones of conduction block, which may predispose to reentry. Activation delays of up to 120 ms were observed over distances as small as 3 mm. Under pathological conditions including stretch and increased fibrosis, these delays may become larger and result in microreentry, which could trigger atrial fibrillation or lead to fibrillatory conduction. The observation that conduction delay occurs at sites that reveal sudden changes in fiber direction is very similar to observations made by Spach and coworkers.[6] These investigators showed that at sites with a sudden change in fiber orientation, an abrupt increase in axial resistivity in the direction of propagation ensued, which resulted in a decrease of the safety factor for propagation. Although abrupt changes in fascicle orientation can explain the delays observed, we cannot rule out that connexin distribution and expression as described by Luke and Saffitz[7] played a role as well.

In addition to reentry, sites with increased axial resistivity may favor the occurrence of ectopic activity. Computer modeling suggests that increased anisotropy favors the exit of activation from a focal source, which is suppressed when anisotropy is normal.[8]

Fractionated Electrograms

In patients, electrograms recorded from the pulmonary veins at sites revealing focal activity are often fractionated and complex, reflecting zones of slow conduction or block. In the present study in canines, they were well correlated with the anatomic fiber arrangement. Spach and Dolber[9] showed that in atrial preparations, anisotropic features of atrial muscle may result in reentrant arrhythmias. In animal models,[10] which include healing and healed myocardial infarction, anisotropic conduction leads to sustained and reentrant tachycardia. Although sustained anisotropic reentry has not been demonstrated conclusively in human atria, the importance of geometric discontinuities is well recognized for reentrant circuits in atrial flutter.

Histology

The present study shows that cells within the pulmonary veins exhibit structural similarities with atrial cells, which is compatible with other studies.[9,11] Using the criteria for histological specialization defined by Aschoff[12] and Monckeberg[13] in 1910, we found that the pulmonary veins did not contain any discrete tracts insulated from the neighboring myocardium or collections of cells that resembled the sinus or atrioventricular node. Masani[14] reported that “clear looking cells” with structural features similar to those of sinus node cells were identified in the intrapulmonary, preterminal portion of the pulmonary vein of the rat heart. Such “pale cells” were also present in some of our preparations (Figure 7). They appeared to resemble damaged cells or cells undergoing ischemic changes. On further investigation, 2 independent pathologists confirmed that these cells appeared to be artifacts.

Intracellular Recordings

In the present study, action potentials did not produce any afterdepolarizations that could lead to triggered activity. Cheung[15] demonstrated that action potentials recorded at the distal end of the pulmonary veins in isolated guinea pig pulmonary veins had a lower amplitude and a shorter duration than cells near the ostium, which is compatible with our results. Cheung also showed that isolated pulmonary veins were capable of independent pace-making activity in cells at the distal end. Cells near the ostium showed stable diastolic potentials between action potentials. Application of norepinephrine accelerated the rate of spontaneously active pulmonary vein preparations. Chen et al[16] recorded spontaneously occurring action potentials at the distal end of the myocardial

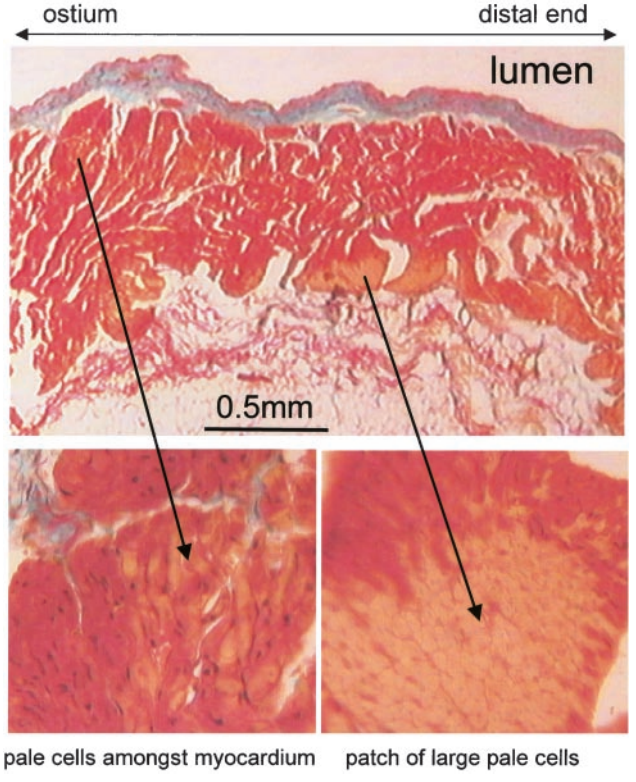

Figure 7. Section illustrating staining artifacts. Pale-staining cells are not specialized but are artifacts that occurred anywhere in the sections, to varying degrees.

sleeves of pulmonary veins of the dog heart. Spontaneously occurring activity was seen in none of our preparations. This is not in contradiction to the study by Cheung[15] because automaticity was absent in his study when the pulmonary vein was electrically coupled to the atrium, as was the case in our preparations. In the study by Chen et al,[16] pulmonary veins were harvested from dog hearts after 6 to 8 weeks of rapid atrial pacing, and preparations were superfused. Differences in the preparations and techniques may well account for the differences in automaticity.

Clinical Implications and Limitations

Electrograms recorded in our animal model are similar to those recorded in patients with lone paroxysmal atrial fibrillation as demonstrated by Haïssaguerre et al.[3] However, we used normal canine hearts, and one can speculate that in aged and diseased atria with extremely slow and fragmented conduction due to nonuniform anisotropy, arrhythmogenicity may be favored. Increased anisotropy may facilitate reentry, but it also affects the initiation of a propagating wave from an ectopic focus.

In dog hearts in the present study, the electrophysiological and histological characteristics did not differ among the veins studied. However, diameters of the right inferior pulmonary veins were too small and myocardial sleeves too short to permit extracellular measurements and adequate microelectrode impalements. These limitations of the study restrict the translation of our data to human pulmonary veins.

Conclusions

Electrophysiological analysis shows that zones of activation delay correlating with histological assessment of myofiber arrangement and distribution are prominent in canine pulmonary veins and suggests that microreentry could occur or promote the exit of activation from a focal source. Although we did not observe complete reentry circuits, reentry might be anticipated to occur under pathological conditions, in which anisotropy is expected to be more pronounced. No evidence of abnormal automaticity or triggered activity was observed.

Acknowledgments

Dr Hocini is supported in part by a grant of the Fédération Française de Cardiologie. Dr Ho is supported by the British Heart Foundation.

References

1. Moe GK, Abildskov JA. Atrial fibrillation as a self-sustaining arrhythmia independent of focal discharge. *Am Heart J*. 1959;58:59–70.
2. Allessie MA, Lammers WJEP, Bonke FIM, et al. Experimental evaluation of Moe's multiple wavelet hypothesis of atrial fibrillation. In: Zipes DP, Jalife J, eds. *Cardiac Electrophysiology and Arrhythmias*. Orlando, Fla: Grune & Stratton; 1985:265–275.
3. Haïssaguerre M, Jaïs P, Shah DC, et al. Spontaneous initiation of atrial fibrillation by ectopic beats originating in the pulmonary veins. *N Engl J Med*. 1998;339:659–666.
4. McGuire MA, de Bakker JMT, Vermeulen JT, et al. Origin and significance of double potentials near the atrioventricular node: correlation of extracellular potentials, intracellular potentials and histology. *Circulation*. 1994;89:2351–2360.
5. Liu Y, Cabo C, Salomonsz R, et al. Effects of diacetyl monoxime on the electrical properties of sheep and guinea pig ventricular muscle. *Cardiovasc Res*. 1993;27:1991–1997.
6. Spach MS, Miller WT Jr, Dolber PC, et al. The functional role of structural complexities in the propagation of depolarization in the atrium of the dog: cardiac conduction disturbances due to discontinuities of effective axial resistivity. *Circ Res*. 1982;50:175–191.
7. Luke RA, Saffitz JE. Remodeling of ventricular conduction pathways in healed canine infarct border zones. *J Clin Invest*. 1991;87:1594–1602.
8. Wilders R, Wagner MB, Golod DA, et al. Effects of anisotropy on the development of cardiac arrhythmias associated with focal activity. *Pflugers Arch*. 2000;441:301–312.
9. Spach MS, Dolber PC. Relating extracellular potentials and their derivatives to anisotropic propagation at a microscopic level in human cardiac muscle: evidence for electrical uncoupling of side-to-side connections with increasing age. *Circulation*. 1986;58:356–371.
10. Dillon S, Allessie MA, Ursell PC, et al. Influence of anisotropic tissue structure on reentrant circuits in the subepicardial border zone of subacute canine infarcts. *Circ Res*. 1988;63:182–206.
11. De Almeida OP, Böhm GM, Carvalho MP, et al. The cardiac muscle in the pulmonary vein of the rat: a morphological and electrophysiological study. *J Morphol*. 1975;145:409–434.
12. Aschoff L. Referat über die Herzstörungen in ihren Beziehungen zu den Spezifischen Muskelsystem des Herzens. *Verh Dtsch Ges Pathol*. 1910; 14:3–35.
13. Monckeberg JG. Beiträge zur normalen und pathologischen Anatomie des Herzens. *Verh Dtsch Ges Pathol*. 1910;14:64–71.
14. Masani F. Node-like cells in the myocardial layer of the pulmonary vein of rats: an ultrastructural study. *J Anat*. 1986;145:133–142.
15. Cheung DW. Electrical activity of the pulmonary vein and its interaction with the right atrium in the guinea-pig. *J Physiol*. 1980;314:445–456.
16. Chen YJ, Chen SA, Chang MS, et al. Arrhythmogenic activity of cardiac muscle in pulmonary veins of the dog: implication for the genesis of atrial fibrillation. *Cardiovasc Res*. 2000;48:265–273.